TOXICOLOGICAL SCIENCES **115(2)**, 521–534 (2010)
doi:10.1093/toxsci/kfq076
Advance Access publication March 10, 2010

Effects of Aqueous Exposure to Silver Nanoparticles of Different Sizes in Rainbow Trout

Tessa M. Scown,* Eduarda M. Santos,* Blair D. Johnston,* Birgit Gaiser,† Mohammed Baalousha,‡ Svetlin Mitov,‡ Jamie R. Lead,‡ Vicki Stone,† Teresa F. Fernandes,† Mark Jepson,§ Ronny van Aerle,*[,1] and Charles R. Tyler*[,1,2]

*Ecotoxicology and Aquatic Biology Research Group, Hatherly Laboratories, School of Biosciences, University of Exeter, Exeter EX4 4PS, UK; †School of Life Sciences, Faculty of Health, Life & Social Sciences, Edinburgh Napier University, Edinburgh EH10 5DT, UK; ‡School of Geography, Earth, and Environmental Sciences, University of Birmingham, Edgbaston, Birmingham B15 2TT, UK; and §Department of Biochemistry, School of Medical Sciences, University of Bristol, University Walk, Bristol BS8 1TD, UK

[1] Joint senior authors.
[2] To whom correspondence should be addressed. Fax: +44-1392-263434. E-mail: c.r.tyler@exeter.ac.uk.

Received November 23, 2009; accepted March 1, 2010

Despite increasing application of silver nanoparticles (NPs) in industry and consumer products, there is still little known about their potential toxicity, particularly to organisms in aquatic environments. To investigate the fate and effects of silver NPs in fish, rainbow trout (*Oncorhynchus mykiss*) were exposed via the water to commercial silver particles of three nominal sizes: 10 nm (N_{10}), 35 nm (N_{35}), and 600–1600 nm (N_{Bulk}), and to silver nitrate for 10 days. Uptake into the gills, liver, and kidneys was quantified by inductively coupled plasma-optical emission spectrometry, and levels of lipid peroxidation in gills, liver, and blood were determined by measurements of thiobarbituric acid reactive substances. Expression of a suite of genes, namely *cyp1a2*, *cyp3a45*, *hsp70a*, *gpx*, and *g6pd*, known to be involved in a range of toxicological response to xenobiotics was analyzed in the gills and liver using real-time PCR. Uptake of silver particles from the water into the tissues of exposed fish was low but nevertheless occurred for current estimated environmental exposures. Of the silver particles tested, N_{10} were found to be the most highly concentrated within gill tissues and N_{10} and N_{Bulk} were the most highly concentrated in liver. There were no effects on lipid peroxidation in any of the tissues analyzed for any of the silver particles tested, and this is likely due to the low uptake rates. However, exposure to N_{10} particles was found to induce expression of *cyp1a2* in the gills, suggesting a possible increase in oxidative metabolism in this tissue.

Key Words: **silver; rainbow trout; lipid peroxidation; nanoparticles; nanotoxicology; gene expression.**

Current growth in the nanotechnology industry and the increasing numbers of products making use of the unusual properties of engineered nanoparticles (NPs) is becoming extremely important in the global economy. Increased production and use of nanoproducts will inevitably lead to increased levels of discharge of nanomaterials into the environment through their intentional and accidental releases or via weathering of products that contain them. The aquatic environment is particularly vulnerable as it is likely to act as a sink for many of these particles, as it does for many chemical discharges. The fate of NPs in the aquatic environment, their interactions with biotic and abiotic components, and their potential to cause harm are all still poorly understood, and these uncertainties are driving concerns on the risks they may pose to human and environmental health. Silver NPs are already used in a variety of consumer products, notably for their antimicrobial properties, including in washing machines (Jung *et al.*, 2007) and fabrics (Perelshtein *et al.*, 2008), and prospective applications also include use in wound dressings (Arora *et al.*, 2008), water treatment filters (Li *et al.*, 2008), catalysts (Kumar *et al.*, 2008), sensors (Schrand *et al.*, 2008), inks (Wang *et al.*, 2008), and pharmaceuticals (Chen and Schluesener, 2008; Sun *et al.*, 2008).

Though their antimicrobial properties are well known (Choi *et al.*, 2008; Jayesh *et al.*, 2008), silver NPs have also been shown to cause toxicity in vertebrate cell lines with findings typified by the generation of reactive oxygen species (ROS) (Hussain *et al.*, 2005; Schrand *et al.*, 2008), apoptosis (Braydich-Stolle *et al.*, 2005; Park *et al.*, 2007), increased lipid peroxidation (Arora *et al.*, 2008), reduced mitochondrial function (Braydich-Stolle *et al.*, 2005; Hussain *et al.*, 2005; Schrand *et al.*, 2008), and depletion of oxidative stress markers (Arora *et al.*, 2008; Hussain *et al.*, 2005). Furthermore, a recent study by Larese *et al.* (2009) demonstrated absorption of silver NPs in the "stratum corneum" and the outermost surface of the epidermis in both intact and damaged human skin.

A few *in vivo* studies in fish have shown some evidence of enhanced toxicity compared with bulk counterparts (i.e., larger particulate silver material > 100 nm). Concentration-dependent mortality and developmental effects, including spinal deformities and cardiac arrhythmia, have been shown in zebrafish

(*Danio rerio*) embryos exposed to silver NPs (5–20 nm) at a threshold concentration of 50 μg/ml (Asharani *et al*., 2008; Yeo and Kang, 2008). In adult zebrafish, exposure to 20- to 30-nm silver NPs has shown a greater toxicity compared with dissolved silver (Ag^+ from silver nitrate), based on mass of metal (Griffitt *et al*., 2009). In that work, more silver was associated with the gills in exposures to NPs (26.6 ± 8.8 nm; 1000 μg/l) compared with fish exposed to silver ions, and there was a greater thickening of the gill filaments in the silver NP–exposed fish compared with controls.

The mechanism of toxicity of silver NPs in fish has not been determined. An enhanced toxicity of nanoparticulate silver, compared to silver ions (Ag^+), may result from their shape and/or size, the release of silver ions (silver ions are well known to be toxic to aquatic organisms) (Mayer *et al*., 2003; Walker *et al*., 2008; Wood *et al*., 1996a), or a combination of both. Navarro *et al*. (2008) examined the rate of photosynthesis in *Chlamydomonas reinhardtii* exposed to silver NPs or silver ions in both the presence and the absence of cysteine (which binds free silver ions) and showed that silver NPs were more toxic than silver ions, based on the concentration of ions present, requiring a higher concentration of cysteine to eliminate the toxicity. These findings suggest that interactions between the algae and the NPs may enhance the release of silver ions, in turn suggesting that the NPs acted as an effective delivery vehicle for silver ions.

Environmental concentrations of silver NPs have not been determined but estimates in natural waters range between 0.03 and 500 ng/l (Luoma, 2008). Sock fabrics are potentially a major source of silver NPs to the aquatic environment; Benn and Westerhoff (2008) showed that washing of socks impregnated with nanoparticulate silver resulted in the release of up to 1300 μg silver/l, some of it nanoparticulate. Many factors will likely affect the relative toxicity of NPs for exposed organisms in natural waters, through effects on aggregation behavior and thus their bioavailability, including pH and ionic concentrations, and interactions between NPs and organic material and natural colloids (Baalousha *et al*., 2008; Handy *et al*., 2008b). Solubility is an important consideration in the toxicity of silver NPs too, and factors affecting their solubility, such as presence of algae (Navarro *et al*., 2008), are also likely to influence this. It is not known how, or indeed if, the release of the silver ions is influenced by the size of the silver particle.

Previous work examining the toxicity of silver NPs has provided conflicting evidence on the influence of size of particle on toxicity. A study by (Carlson *et al*., 2008) exposing alveolar macrophages to silver NPs found that the generation of ROS was size dependent. Inoue *et al*. (2009) also found that particle size was a determining factor in the level of lung inflammation in mice exposed to latex NPs. However, in a series of pulmonary instillation studies in rats with nanoscale TiO_2 rods and dots, Warheit *et al*. (2006) did not find that toxicity to the pulmonary system was dependent on either particle size or surface area. Contrasting with this, however, a further study by this research group (Warheit *et al*., 2007) found that the surface characteristics of quartz particles were responsible for the differences in pulmonary toxicity. There may, of course, be particle type–specific effects. That is, nanoscale may increase the inherent toxicity of some materials but not others.

The purposes of our study were twofold. First, to investigate the fate and effects of silver NPs in rainbow trout exposed via the water column, including at concentrations with likely environmental relevance, and second, to investigate any differences in the fate and biological effects due to the size of the particle. We exposed juvenile rainbow trout to three nominal sizes of silver particle: 10 nm (N_{10}), 35 nm (N_{35}), and 600–1600 nm (N_{Bulk}) and to silver nitrate for 10 days and measured the silver concentration in the gills, liver, and kidney. Thiobarbituric acid reactive substances (TBARS) were measured in the blood plasma and in gill and liver tissue homogenates to ascertain whether lipid peroxidation had occurred as a result of exposure. Furthermore, expression of a suite of genes related to metabolism and response to xenobiotics, specifically glucose-6-phosphate dehydrogenase (*g6pd*), glutathione peroxidase (*gpx*), cytochrome P450 1A2 (*cyp1a2*), cytochrome P450 3A45 (*cyp3a45*), and heat-shock protein 70a (*hsp70a*), were analyzed in the gills and liver as additional biological effect measures reporting on specific mechanisms of toxicity. Previous studies have shown the expression of these genes to be upregulated in rainbow trout (Lee and Buhler 2003; Råbergh *et al*., 2000; Walker *et al*., 2007; Williams *et al*., 1996) and brown trout (Hansen *et al*., 2006, 2007) in response to exposure to various metals.

MATERIALS AND METHODS

Rainbow trout husbandry. Juvenile female rainbow trout with a mean total body weight of 19.52 ± 0.56 g (mean ± SE) and fork length of 12.39 ± 0.14 g (mean ± SE) were obtained from Hatchlands Trout Farm (Devon, UK). Fish were maintained in the laboratory in 500-l tanks supplied via a flow-through system with dechlorinated tap water (pH 7.79 ± 0.01 [SE] and conductivity 189.58 μs ± 0.49 [SE]) on a 12-h light/12-h dark cycle and were fed on pelleted feed (Emerald Fingerling 30; Skretting, UK), at a rate of 1% of their body weight prior to exposure. Water temperatures were maintained between 9°C and 11°C throughout.

Materials and particle characterization. All chemicals were purchased from Sigma-Aldrich, UK, unless otherwise stated. Silver particles (designated as N_{10}, N_{35}, and N_{Bulk}) were purchased from Nanostructured and Amorphous Materials Inc. (Houston). Based on the manufacturers specifications, N_{10} (average particle size measured by transmission electron microscopy [TEM]) silver particles were spherical particles with a specific surface area of 9–11 m^2/g, bulk density of 2.05 g/cm^3 and a true density of 10.5 g/cm^3, and had a purity of 99.9% based on trace metal analysis. N_{35} silver particles of average size 35 nm (measured by TEM; max < 100 nm) had a specific surface area of 30–50 m^2/g, bulk density of 0.30–0.60 g/cm^3 and a true density of 10.5 g/cm^3, and had a purity of 99.5% based on trace metal analysis. N_{Bulk} silver particles had an average particle size of 0.6–1.6 μm and purity of 99.95%.

Our own characterization of all the silver particles was carried out in high performance liquid chromatography (HPLC)-grade water or on powders. Particle sizes (hydrodynamic diameters), polydispersity index, and zeta potential were measured on a Zetasizer Nano ZS ZEN3600 (Malvern

Instruments Ltd, Malvern, UK) operating with a He-Ne laser at a wavelength of 633 nm using back-scattered light. Our results are the means of triplicate runs, and in each run, five measurements were made and SEs were determined from the replicate measurements. Particle sizes and particle numbers were also measured using a NanoSight NTA LM10 with a laser output of 30 mW at 650 nm. Mean square displacements of single particles were determined by tracking the scattered light followed by analysis by the Nanosight software, and SDs of the mean values were calculated. All measurements were carried out at NP concentrations of 1 mg/l after sonication for 30 min. The adsorption method was used to prepare samples for atomic force microscopy (AFM) analysis. In this method, mica sheets were cleaved on both sides and then immersed vertically into the sample solution (10 mg/l) for 30 min (in the case of N_{Bulk}, both 30 min and 4 h were tested). Following adsorption, the mica sheets were withdrawn from the solution and gently rinsed by immersion in deionized water to remove nonadsorbed sample. All AFM images were obtained using a XE-100 AFM (Park Systems). All scans were performed in air, at room temperature, and AFM height measurements were recorded. Images were acquired in a true noncontact mode and recorded in topography mode with a pixel size of 256 × 256 and a scan rate of 0.5–1.0 Hz. Eighty particles were counted in case of N_{10}, 40 particles were counted in case of N_{35}, and 10 particles in case of N_{Bulk}, and mean particle sizes including SEs are reported. The low counts reflected the absence of particles on the mica. X-ray diffraction (XRD) was performed using a Bruker AXS D8 Autosampler. EVA software program was used for the assignment of reflections and analysis of the XRD patterns. Crystallite sizes were evaluated using the Scherrer equation, and mean SE values are reported. A JEOL JSM-7000F Field Emission Scanning Electron Microscope was employed to characterize particle size, and back-scattered electron images were recorded. Air drying of a small drop of suspension directly onto a Formvar/Carbon 300 mesh Ni grid was employed.

An FEI TECNAI F20 field emission gun (FEG) coupled with an X-ray Energy Dispersive Spectrometer from Oxford Instruments (Oxfordshire, UK) was used for TEM particle size analysis. The TEM was operating at an accelerating voltage of 200 keV, an FEG at emission 3, gun lens 2–3 (apparent size), and extraction voltage of 3800–4400 eV and spot size 2–3. The aperture of the second condenser lens was nominally 50 μm, and the objective aperture was nominally 40 μm. TEM micrographs were collected on a Gatan TV camera, and Digital Micrograph software was used to measure particle size. TEM samples were prepared by ultracentrifugation of NP suspensions on a TEM grid at 30,000 rpm (150,000 × g) using a Beckman ultracentrifuge (L7-65 Ultracentrifuge) with a swing out rotor SW40Ti as described in Wilkinson *et al*. (1999).

Brunauer, Emmett, and Teller (BET) surface areas (m^2/g) were determined on a Coulter SA3100 series surface area and pore size analyzer. Samples were outgassed for 10 h at 200°C prior to analysis. Results are the means of three measurements, and the SEs are reported.

Experimental design. Eight fish were deployed into experimental glass tanks measuring 60 × 30 × 38 cm (L × W × H) with a total volume of 36 l, and aerated with 10-cm airstones. Seven treatment regimes were run in duplicate and these were as follows: 10 μg/l N_{10} silver particles (N_{10} Low), 100 μg/l N_{10} silver particles (N_{10} High), 10 μg/l N_{35} silver particles (N_{35} Low), 100 μg/l N_{35} silver particles (N_{35} High), 100 μg/l N_{Bulk} silver particles (N_{Bulk}), 0.1 μg/l silver nitrate ($AgNO_3$), and water control. Fish were exposed for 10 days and were not fed for the duration of the exposure.

Dosing stocks of the silver particles were made by suspending 360 mg of each particle in 1 l ultrapure water (Maxima ultrapure water; Elga) and sonicating for 30 min and diluting as required. The silver nitrate dosing stock (360 μg/l) was also made up in ultrapure water and sonicated similarly. Experimental tanks were dosed 24 h prior to addition of the fish, then drained, and redosed immediately before adding the fish to minimize reduction of nominal dosing concentrations through adhesion of the particles/chemical to the glass and airstones. Water changes of 75% (27 l) and corresponding redosing were carried out every 48 h. Dosing stocks were sonicated for 30 min prior to each dosing.

Water samples (9 ml) were taken immediately after addition of the fish at 1, 2, 4, 8, 12, and 24 h; before and after every water change; and at the end of the exposure for analysis of silver concentration by inductively coupled plasma-optical emission spectroscopy (ICP-OES). Water pH and conductivity were monitored daily and ranged between 7.58–8.54 and 179–212 μs, respectively.

Experimental sampling. At the end of the exposure period (10 days), fish were euthanized with an overdose of benzocaine. One milliliter of blood was taken from each fish and centrifuged at 12,000 × g for 5 min at 4°C and the plasma removed and stored at −20°C for analysis of TBARS. Both gill arches were removed and divided as follows: ~50 mg was taken and flash frozen in liquid nitrogen and stored at −80°C for RNA extraction and subsequent gene expression analysis, ~100 mg was taken and frozen in liquid nitrogen and stored at −20°C for analysis of TBARS, and the remainder was weighed, frozen in 50-ml falcon tubes, and stored at −20°C before preparation for measurement of silver content using ICP-OES. Additionally, from one fish in each tank, a 4-mm section of gill tissue was taken and fixed in formalin for histopathological analysis. A further 4-mm section was taken from one fish from the N_{10} High treatment and one control fish and fixed in 2% paraformaldehyde/2.5% glutaraldehyde for TEM analysis. The liver was dissected out from each fish, and a 50-mg sample was taken and stored at −80°C for subsequent RNA extraction. In addition, a 100-mg section was taken and stored at −20°C for TBARS analysis, and a 4-mm^3 sample was taken and fixed in formalin for histological processing and tissue effects analysis. The remaining liver tissue was weighed, frozen, and stored at −20°C prior to preparation and analysis for silver content by ICP-OES. Kidneys were dissected out, weighed, frozen, and stored at −20°C for analysis of silver content via ICP-OES.

Determination of silver concentrations in fish tissues. Tissue and blood samples were defrosted and digested at room temperature with a combination of 4 ml concentrated HNO_3 (AR grade; Fisher Scientific) and 1 ml hydrogen peroxide (Laboratory reagent grade; Fisher Scientific) for 24 h before being heated for 24 h on a Gerhardt Kjeldatherm digester unit at 125°C. The temperature was then increased to 190°C to evaporate the nitric acid, and the samples were subsequently redissolved in 10 ml of 10% HNO_3 and 200 μl of 10% Triton-X 100. The samples were then analyzed on a Vista-MPX CCD Simultaneous ICP-OES. Water samples were prepared for analysis by the addition of 1 ml HNO_3 and 200 μl of 10% Triton-X 100. Calibration standards containing 500 μg/l and 1000 μg/l and a quality control standard containing 400 μg/l silver were made up from a stock solution of 157.5 mg/l silver nitrate in 10% HNO_3. Internal standards of 1, 10, 100, 500, and 1000 μg/l were made using all silver particle types suspended in 10% HNO_3 dispersed with 10% Triton-X 100 and used according to the exposure regime samples being measured, i.e., N_{10} internal standards for N_{10} exposure samples. All samples and standards were sonicated for 30 min prior to measurement. The detection limit of the ICP-OES for silver in the tissue and water samples was 10 μg/l.

Histological analyses. Trout liver and gill tissues were fixed in 10% neutral buffered formalin for 6 h before being transferred to 70% industrial methylated spirits (IMS). The tissue samples were dehydrated in series in IMS (AR grade; Fisher Scientific) in a Shandon Hypercenter XP Tissue Processor and embedded in paraffin wax. The samples were sectioned on a rotary microtome (Leica). Five microscope slides, with five to six sections per slide, were prepared for each tissue sample, and the slides were stained with hematoxylin and eosin in a Shandon automatic slide stainer (Thermo Scientific, UK). Tissues were examined and assessed for any signs of histopathological changes using a Zeiss Axioskop 40 light microscope with an Olympus DP70 Digital Microscope Camera and AnalySIS Image Processing Software (Watford, UK) and examined for evidence of gill or liver injury.

Gill tissues were fixed for TEM adopting an in-house method. Briefly, tissues were fixed for 2 h in 2% paraformaldehyde/2.5% glutaraldehyde in 0.1M phosphate buffer (pH 7.4), washed three times in 0.1M phosphate buffer for 5 min, and fixed in 1% osmium tetroxide in phosphate buffer for 1 h. The tissues were then washed in deionized water for 5 × 5 min, before being cut into 1-mm^3 pieces, and subsequently suspended in 2% uranyl acetate for 1 h. The tissues were then dehydrated in an ethanol series: 30, 50, 70, 90, and 100% (×2), in each for 10 min and embedded in TAAB resin. The tissues were

blocked in shallow planchets and placed in a 60°C oven for 20 h. Tissues were sectioned on an ultramicrotome (Ultracut; Reichert) and examined for structural alterations and subcellular localization of silver using a Joel TEM 1400 transmission electron microscope.

Measurement of lipid peroxidation. Measurement of 1,1,3,3-tetramethoxypropane (malonaldehyde [MDA]) using the TBARS assay is widely used as an indicator of lipid peroxidation. The protocol adopted was similar to that described previously (Conner *et al.*, 2006). Briefly, eight standards of MDA at concentrations ranging from 0.625 to 100μM were prepared from a 500μM stock solution of MDA in 2% ethanol. Tissue samples were homogenized with a handheld tissue homogenizer with 250 μl of 100mM 4-(2-hydroxyethyl)-1-piperazineethanesulfonic acid. The samples were then centrifuged at 1600 × g for 10 min at 4°C and the supernatant reserved. Hundred microliters of tissue homogenate/plasma and standards was mixed with 500 μl of 0.4% thiobarbituric acid (40 mg in 10 ml) in 10% acetic acid, pH 5.0. The tubes were heated to 90°C for 1 h and then cooled to room temperature under tap water. Six hundred microliters of butanol was added and the mixture was then vortexed and then centrifuged at 3100 × g for 10 min. The butanol phase was removed, and 150 μl was placed in duplicate in a flat-bottomed 96-well microtiter plate and the absorbance measured at 532 nm on a Molecular Devices SpectraMax 340pc microtiter plate reader. A standard curve was prepared and MDA concentrations were determined accordingly.

Gene expression analyses. Total RNA was extracted from each tissue sample using Tri Reagent (Sigma) following the manufacturer's instructions. Total RNA concentrations were determined by measuring the absorbance at 260 nm using a Nanodrop ND-1000 spectrophotometer (NanoDrop Technologies). The RNA was treated with DNase (Cat. No. M6101; Promega) and subsequently reverse transcribed to complementary DNA (cDNA) using M-MLV Reverse transcriptase (Cat. No. M1701; Promega) and random hexamer primers as previously described (Filby and Tyler, 2005).

Real-time PCR assays were developed for the quantification of a selection of genes involved in the response to xenobiotics and their metabolism in rainbow trout. Primers specific for rainbow trout glucose-6-phosphate dehydrogenase (*g6pd*; GenBank accession no. EF551311: 5′-CGGTTGTCTGTGTTCTTC-3′/5′-GGTGCTTGATGTTCTTGG-3′), glutathione peroxidase (*gpx*; Genbank accession no. AF281338: 5′-GCTCCATTCGCAGTATTC-3′/5′-TCCTTCCC-ATTCACATCC-3′), cytochrome P450 1A2 (*cyp1a2*; Genbank accession no. U62797: 5′-CTTCCGCCATATTGTCGTATC-3′/5′-CCACCACCTGCC-CAAAC-3′), cytochrome P450 3A45 (*cyp3a45*; Genbank accession no. AF267126: 5′-GTCCTCTCACCTTCCTTTACC-3′/5′-TCTGCCTGCTTCTTC-ATTCC-3′), and heat-shock protein 70a (*hsp70a*; Genbank accession no. NM_001124228: 5′-CTGCTGCTGCTGGATGTG-3′/5′-GCTGGTTGTCGG-AGTAAGTG-3′) were designed for use in real-time PCR with Beacon Designer 7.2 software (Premier Biosoft International, Palo Alto, CA) according to manufacturer's guidelines and purchased from MWG Biotech. Assays were optimized and validated for real-time PCR using SYBR Green chemistry as described previously (Filby and Tyler, 2005).

Assays had detection ranges of at least three orders of magnitude. Specificity of primer sets throughout this range of detection was confirmed by the observation of single amplification products of the expected size and melting temperature. All assays were quantitative with standard curve (mean threshold cycle [C_t] vs. log cDNA dilution) slopes of −2.754 (*g6pd*), −3.367 (*gpx*), −2.901 (*cyp1a2*), −2.722 (*cyp3a45*), and −3.538 (*hsp70a*), translating to high PCR efficiencies (E) of 2.31 (*g6pd*), 1.98 (*gpx*), 2.21 (*cyp1a2*), 2.33 (*cyp3a45*), and 1.92 (*hsp70a*). Over the detection range, the linear correlation (R^2) between the mean C_t and the logarithm of the cDNA dilution was > 0.98 in each case.

Gene expression was measured for each gene in liver and gill samples using SYBR Green chemistry with the iCycler iQ Real-time Detection System (Bio-Rad Laboratories, Inc., Hercules, CA) according to the protocols described previously (Filby and Tyler, 2005).

For each gene, samples were analyzed in triplicate. Relative expression levels were calculated using an efficiency-corrected version of the arithmetic comparative $2^{-\Delta\Delta C_t}$ method, as described previously (Filby and Tyler, 2005). The housekeeping gene ribosomal protein L8 (*rpl8*) was also measured in each sample and was used for relative quantification because its expression did not change for the tissues analyzed following any of the treatments.

Statistical analyses. Data are expressed as mean values ± SE of the mean (SE), and statistical analyses were performed using SPSS version 16.0, with the significance value set at 0.05. All data were checked for conformity with the assumptions of normality (normality of error and homogeneity of variance). When these assumptions were not met, data were either transformed to meet these assumptions or equivalent nonparametric tests were conducted (see relevant sections of the "Results" for further details).

RESULTS

Particle Characterization

Particles with zeta potentials more positive than +30 mV or more negative than −30 mV are normally considered stable (Derjaguin and Landau, 1941; Verwey and Overbeek, 1948) in the absence of steric stabilization. If the particles have a higher density than the solution, they will eventually sediment. Zeta potential measurements of all silver particle types in HPLC-grade water suggested that the particles had a high propensity for aggregation (Table 1), which was confirmed by hydrodynamic diameter measurements of the particles. The N_{10} silver particles had the most negative zeta potential value (−12.5 mV), on average formed the smallest aggregate sizes in water (~590 nm, measured by dynamic light scattering [DLS]), and had the lowest polydispersity index, suggesting that aggregate sizes were more uniform compared to the two other particle types. The N_{35} silver formed the largest aggregates in water (~2030 nm) and had a high polydispersity index, suggesting that both larger and smaller aggregate sizes were present. N_{Bulk} silver had an average aggregate size of 940 nm and a polydispersity index of 0.69, suggesting that aggregates were of a more uniform size than for the N_{35} silver particles. Aggregation, followed by sedimentation, would have removed much of the material from the water column limiting potential uptake of the NPs. Furthermore, it might be expected that diffusive uptake into gills would be limited from this aggregation.

Particle sizes determined from nanoparticle tracking analysis (NTA) are lower compared to the values obtained from DLS technique (Table 1), as previously found (Domingos *et al.*, 2009), possibly due to the bias toward large aggregates in DLS. The N_{35} and N_{10} silver particles show similar hydrodynamic diameters from NTA. However, particle number concentrations differ significantly: 1.07×10^8 for the latter and 0.21×10^8 for the former. The higher particle number concentration for the N_{10} silver partly explains the higher tendency for aggregation, as is also observed on back-scattered electron images. It is also clearly seen that the number of smaller particles is higher for the N_{10} particles compared to the N_{35}, giving good agreement with the TEM data (Figs. 1A–C and Table 1). In the case of N_{Bulk} silver, single particles between 1 and 2 μm could be identified alongside smaller particle sizes.

TABLE 1
Size and Charge Characterization Data for Silver Particles Suspended in HPLC-Grade Water

	N_{10} silver	N_{10} silver manufacturers specifications	N_{35} silver	N_{35} silver manufacturers specifications	N_{Bulk} silver	N_{Bulk} silver manufacturers specifications
Zeta potential (mV)	−12.52 ± 2.7	—	−6.5 ± 1.8	—	−2.8 ± 0.6	—
pH	7.11	—	7.34	—	6.40	—
Hydrodynamic diameter (nm) (DLS)	589 ± 101	—	2029 ± 524	—	938 ± 230	—
Polydispersity index	0.54	—	0.93	—	0.69	—
Hydrodynamic diameter (nm) (NTA technique)	158 ± 76	—	166 ± 72	—	217 ± 130	—
Particle number per ml (NTA technique)	1.07×10^8	—	0.21×10^8	—	0.27×10^8	—
Mean primary particle size (nm) (TEM)	49 ± 18.5	10	114 ± 65.3	35 (max < 100 nm)	137 ± 62.0	600—1600
Mean particle size (nm) (AFM)	46.3 ± 10.7	—	90.0 ± 15.6	—	147.5 ± 82.3	—
Crystallite size (nm) (XRD technique)	21.2 ± 0.5	—	68.0 ± 2.0	—	60.0 ± 4.6	—
Surface area (m^2/g) (BET)	2.0 ± 0.2	9–11	2.9 ± 0.2	30–50	0.6 ± 0.1	—
Bulk density (g/cm^3)	—	2.05	—	0.3–0.6	—	—
True density (g/cm^3)	—	10.5	—	10.5	—	—
Purity (trace metal analysis)	—	99.9%	—	99.5%	—	99.95%

Ag crystallite sizes were calculated using the Scherrer equation from XRD spectra. As expected and in agreement with the Bragg peak broadening of the XRD patterns (Fig. 1D), the N_{10} silver showed the smallest crystallite size (21 nm), indicated by the peak broadening in the XRD data, not seen for the larger-sized particles. However, N_{35} silver and N_{Bulk} silver showed similar crystallite sizes (68 and 60 nm, respectively), suggesting that the N_{35} silver contains mainly large particles similar to the N_{Bulk} particles (also observed by TEM imaging; Figs. 1E–G). XRD analysis confirmed cubic crystal system (face-centered lattice) in case of all the three silver samples.

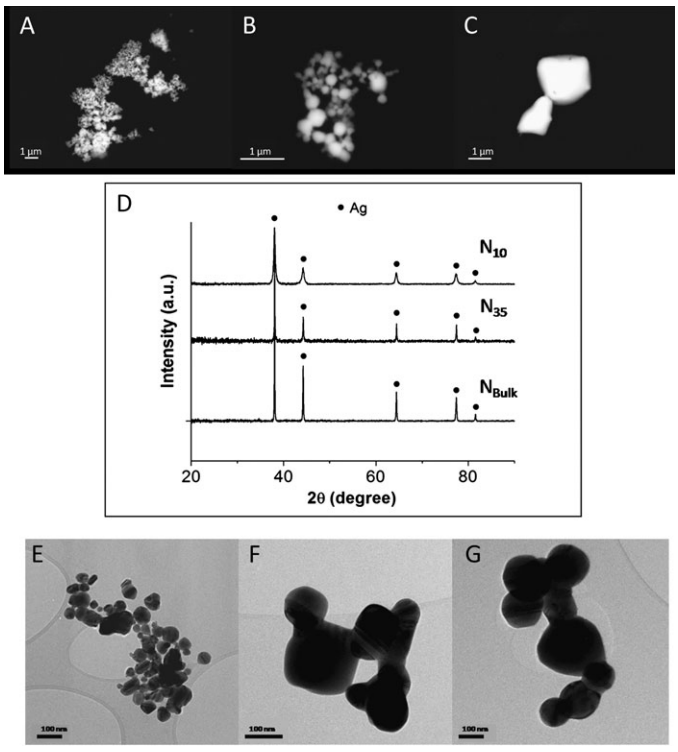

FIG. 1. Characterization of silver particles: back-scattered electron images obtained from (A) N_{10}, (B) N_{35}, and (C) N_{Bulk} silver particles, (D) XRD pattern for silver particles and TEM images obtained from (E) N_{10}, (F) N_{35}, and (G) N_{Bulk} silver particles.

Semiquantitative AFM analysis showed the presence of small particles with approximate sizes of 46 nm in the case of N_{10} silver, giving very good agreement with TEM data (Table 1). However, single large particles/aggregates between 140 and 190 nm were also identified in agreement with NTA data. In the case of N_{35} silver, particles with approximate sizes of 90 nm were identified together with larger particles/aggregates between 130 and 140 nm, giving good agreement with both TEM and NTA data. Smaller particles of approximate size of 10 nm were also observed, again confirming the sample polydispersity and giving good agreement with the NTA data. In the case of N_{Bulk} silver (30-min adsorption time), only smaller particles of an approximate size of 18 nm were observed, suggesting that larger particles were not sticking to the mica slide support due to low diffusivities and low adhesion to the mica. However, the bulk particle sample clearly contained very small nano-sized particles, although in much lower concentrations, than the N_{10} and N_{35} samples. In addition, the 4-h adsorption time employed for N_{Bulk} silver identified particles with approximate sizes of 147 nm, but very small particles (~18 nm) were also observed in this sample.

The BET method was used for determining Ag-specific surface areas. The measured BET surface area values are lower than those supplied by manufacturer (Table 1) but in agreement with all the measured size data. The low values observed are consistent with both the larger particles observed and the possibility of reduced specific surface areas as NPs become densely packed and aggregated during outgassing. As expected,

the smallest surface area (0.6 m^2/g) was obtained for the N_{Bulk}, while N_{10} and N_{35} showed similar specific surface areas (2.0 and 2.9 m^2/g, respectively). Synthesis of all data indicates that the N_{10} particles were clearly smaller than the N_{35} particles and these were smaller than the N_{Bulk} particles. Nevertheless, there was considerable sample polydispersity.

TEM analysis suggests that the N_{10} and N_{35} particles are larger than reported by the manufacturer with an average diameter of 49 ± 18.5 and 114 ± 65.3 nm, respectively, whereas the N_{Bulk} particles are smaller than reported by the manufacturer with an average diameter of 137.4 ± 62.2 nm (Table 1). The N_{10} sample contained only particles < 100 nm, whereas the N_{35} and N_{Bulk} samples contained a high proportion of large particles with 47 and 75.6%, respectively, being larger than 100 nm. Additionally, the N_{10} sample contained a high proportion (51%) of particles, < 50 nm, whereas the N_{35} and N_{Bulk} samples contained a very small fraction (11.6 and 1.4% respectively) of these particles. TEM analyses indicate that the N_{10} sample was different from the other two samples, which are very similar in terms of their size as determined by TEM.

Exposure Media and Tissue Silver Content

Trace metal analysis of water samples taken from the exposure tanks by ICP-OES showed that the measured silver concentrations in the water were considerably lower for all exposure conditions except for the N_{35} Low concentration treatment. Silver concentrations in the N_{10} Low and $AgNO_3$ tanks were below the detection limit of the ICP-OES machine for all samples. For the N_{10} High, N_{35} Low, N_{35} High, and N_{Bulk} treatments, the mean silver concentrations in the exposure media were 35.5 µg/l ± 2.44 (SE), 9.4 µg/l ± 4.62 (SE), 35.3 µg/l ± 2.64 (SE), and 46.6 µg/l ± 4.73 (SE), respectively.

Trace metal analysis of the trout tissues determined by ICP-OES showed that there was significantly enhanced level of silver in/on the gills of fish in all treatments compared with controls, except for the $AgNO_3$ exposure, where the $AgNO_3$ dose to the tanks was between 100- and 1000-fold lower than the engineered nanoparticle (ENP) concentrations (Fig. 2). The highest concentration of silver was observed in the gills of fish in the N_{10} High treatment group with an average of 0.61 ± 0.07 µg/g tissue (mean ± SE), and this was significantly higher (Mann-Whitney with Holm's Sequential Bonferroni Adjustment $U(4) = 37.00, Z = -3.43, p < 0.001$) compared with in the gills of fish from the N_{10} Low treatment, where the concentrations were ~50% lower. Similar mean silver concentrations were observed in the gills of fish in the N_{35} Low (0.26 µg/g tissue ± 0.06 µg/g), N_{35} High (0.25 µg/g tissue ± 0.08 µg/g), and the N_{Bulk} treatments (0.32 µg/g tissue ± 0.21 µg/g).

Analysis of the liver revealed silver uptake in all four treatment groups: N_{10} High, N_{35} Low, N_{35} High, and N_{Bulk}. The highest uptake occurred in the liver of fish exposed to N_{Bulk} silver particles at 1.63 ± 0.18 µg/g tissue compared with 1.50 ± 0.30 µg/g tissue in the N_{10} High and 0.92 ± 0.16 µg/g

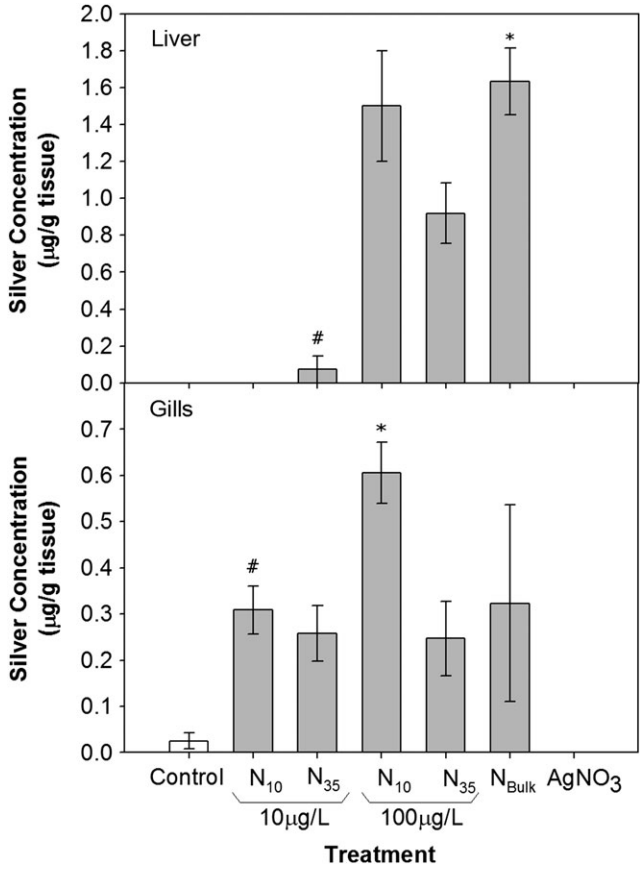

FIG. 2. Concentrations of silver in gills and liver of rainbow trout after waterborne exposure to N_{10}, N_{35}, and N_{Bulk} silver particles and silver nitrate. Data are means ± SE; $n = 8$ per treatment. Liver, #significantly lower than N_{10} High, N_{35} High, and N_{Bulk} (Mann-Whitney $p < 0.001$) and *significantly higher than N_{35} High (Mann-Whitney $p < 0.001$). Gills, #significantly lower than N_{10} Low (Mann-Whitney $p < 0.001$) and *significantly higher than N_{35} Low, N_{35} High, and N_{Bulk} (Mann-Whitney $p = 0.001$).

tissue in the N_{35} High treatment groups. The uptake of N_{Bulk} particles into the liver was significantly higher than the uptake of the N_{35} High treatment group (Mann-Whitney with Holm's Sequential Bonferroni Adjustment $U(3) = 64.00, Z = -2.414, p = 0.015$). There was a small amount of hepatic uptake of N_{35} particles in the low exposure treatment, but this occurred in one fish only. No uptake was detected in the liver of fish exposed to $AgNO_3$ or the N_{10} Low treatment groups. Where uptake of silver into the liver occurred, the overall silver content was more than double the levels in the gill tissue in those fish. Levels of silver in the kidneys of exposed fish were below the detection limit for all treatments.

Lipid Peroxidation

Analysis of TBARS showed no evidence of lipid peroxidation in the gills of fish from any of the treatments, except for the N_{10} High treatment (that contained the highest gill silver content), with significantly lower levels of measured MDA compared with controls (ANOVA with Tukey's *post hoc* test;

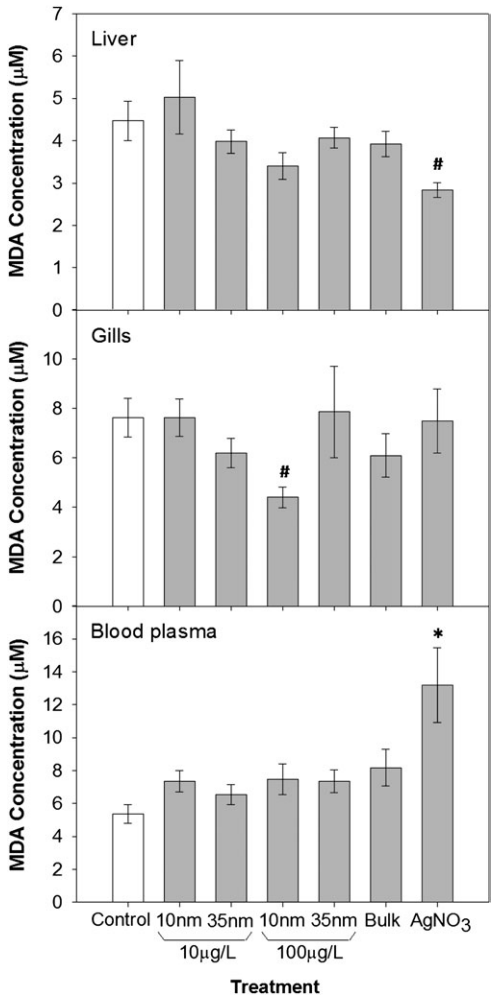

FIG. 3. TBARS in liver and gill tissue homogenates and plasma of rainbow trout after waterborne exposure to N_{10}, N_{35}, and N_{Bulk} silver particles and silver nitrate. Data are means ± SE; $n = 8$ per treatment. Liver, significantly lower than Control, N_{10} Low, N_{35} Low, and N_{35} High (Tukey's $p = 0.001$). Gills, #significantly lower than control and N_{10} Low (Tukey's $p = 0.021$). Plasma, *significantly higher than control, N_{10} Low, and N_{35} Low (Tukey's $p = 0.001$).

$df = 6,104$, $F = 2.629$, $p = 0.021$) (Fig. 3). In the liver tissue homogenates, similarly, there was no evidence of lipid peroxidation, except for MDA concentrations in the livers of the fish from the silver nitrate treatment, which were significantly lower compared with those in the controls (ANOVA with Tukey's *post hoc* test; $df = 6,105$, $F = 3.993$, $p = 0.001$). Examination of TBARS in the blood plasma showed no evidence of an elevation in MDA concentration for any of the particle treatment groups. There was, however, evidence of lipid peroxidation in the plasma of fish from the silver nitrate treatment, where MDA concentrations were significantly higher than controls, and the N_{10} Low and N_{35} Low treatment groups (ANOVA with Tukey's *post hoc* test; $df = 6,90$, $F = 3.991$, $p = 0.001$).

Histology

Histological examination of gill tissue showed no evidence of physical damage or changes to gill filaments in treatments to silver for any of the particle sizes. Gills of fish exposed to $AgNO_3$, however, showed slight damage with deformation of the secondary lamellae observed (Fig. 4). There was no evidence of tissue damage in the liver for any of the silver treatments compared with controls (data not shown).

TEM Analysis

Micrographs of gill tissue from N_{10} High treatment show electron dense areas, which correspond to particles associated with the gill tissue. The particles are highly aggregated in clusters of ~600 nm, corresponding well with the hydrodynamic diameter size as measured by dynamic light scattering (~590 nm) and appear to be associating with the pavement cells at the gill surface (Fig. 5). There was no confirmation of the presence of silver in the gill tissue by energy-dispersive X-ray spectroscopy (EDX) analysis (data not shown). However, Ag content of the tissue must be ~0.1% or greater in order to be detected using this method.

Quantitative Real-Time PCR

Analysis of the expression of five genes that have been shown previously to be induced in rainbow trout gills and liver as a result of exposure to various metal ions showed that their expression was unchanged as a result of exposure to silver particles, with the exception for *cyp1a2*, where there was a threefold induction in the gills of fish exposed to the high concentration of N_{10} particles (ANOVA: $df = 6,48$, $F = 2.691$, $p = 0.025$) (Fig. 6).

DISCUSSION

Very few studies to date have investigated the effects of exposure to silver NPs in fish, and these have been focused on zebrafish embryos where mortality, notochord, and heart abnormalities have all been described (Asharani *et al.*, 2008; Lee *et al.*, 2007; Yeo and Kang, 2008). Similarly, there is little in the literature regarding the uptake and biodistribution of silver NPs into internal organs or the potential toxicity of silver NP in intact free-swimming fish. Furthermore, there have been no studies in fish examining the differential uptake and toxicity of nano-sized versus bulk-sized silver particles. The main aims of this study were, therefore, to identify the target organs for silver particles of different sizes as a result of *in vivo* exposure and uptake from the water in fish, using rainbow trout as a study species, and to compare the patterns of biodistribution and toxicological effects seen for two different sized silver NPs (nominally 10 and 35 nm) and bulk silver particles (nominally 600–1600 nm).

There was clearly a substantial difference between the manufacturer's information on material properties and those

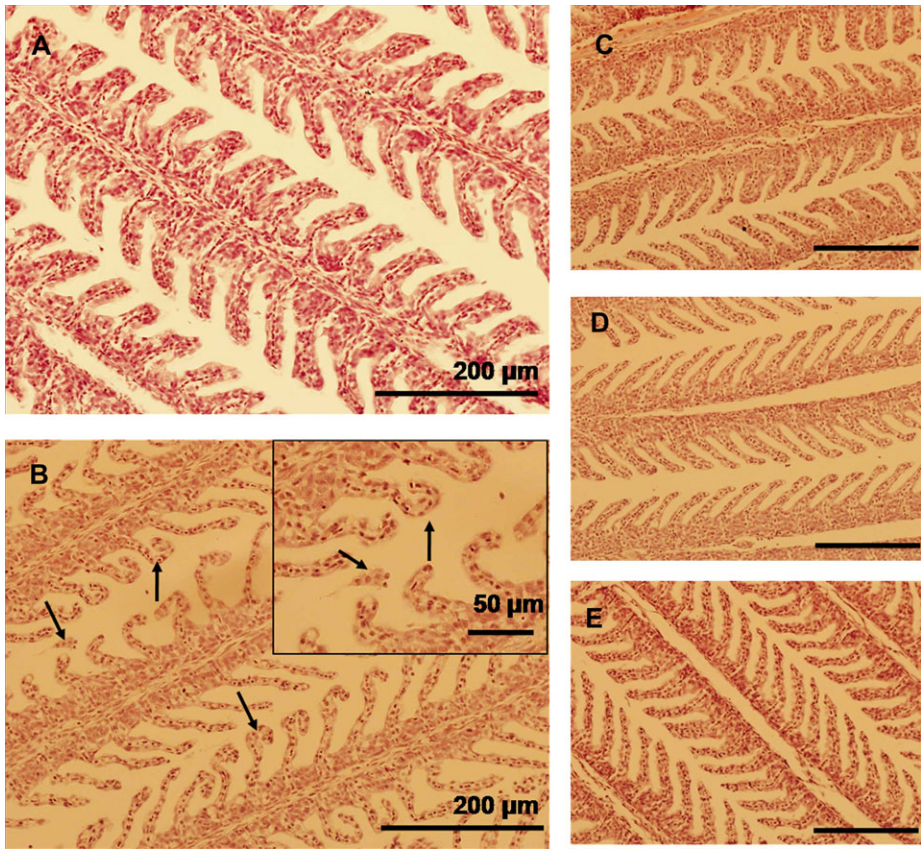

FIG. 4. Gill morphology as visualized by light microscopy in rainbow trout after 10-day waterborne exposure to silver particles and silver nitrate. (A) Control, (B) 0.1 µg/l $AgNO_3$ with close-up inset of damage, (C) 100 µg/l N_{10} silver particles, (D) 100 µg/l N_{35} silver particles, and (E) 100 µg/l N_{Bulk} silver particles. Arrows indicate damage to secondary lamellae.

seen by our own investigations. This discrepancy has been observed by many workers and leads us to the strong recommendation that, as a minimum, commercially obtained NPs need to be fully characterized before any toxicology or other experiments are performed. The reasons for the differences are most likely to be (1) incorrect manufacturer's information, possibly due to limited and/or inappropriate measurement or batch-to-batch variation or (2) changes in material properties between synthesis and initial characterization and use. The characterization performed here in the silver particles is internally consistent, showing that all three particles are polydisperse, with the NPs generally larger than their nominal values and existing, at least partially, as nanostructured aggregates. The larger particles were generally better characterized by the manufacturer, but it is noticeable that there were also some small particles present in those samples. Thus, we would expect that all samples would have low (mass) bioavailability and not to behave as well dispersed 10- or 35-nm particles. Nevertheless, the NPs are likely to be representative of commercially available NPs in current commercial products. For all the measurements of silver concentration in the exposure media, except for in the N_{35} Low treatment group, the actual measurements were as much as 65% lower than the nominal dosing concentrations, even immediately after dosing. The silver concentration in the tank water were highest, as expected after the (re)dosing of the tanks during the water changes, and then, they gradually and progressively decreased over time until the next (re)dosing event (data not shown). These data suggest that aggregation and sedimentation of the particles in the exposure media resulted in a lower silver NP concentration in the water column (and to which the fish were being exposed) compared with the nominal dosing concentration. The level of silver in the gills of rainbow trout exposed to the high dose of N_{10} silver particles was significantly higher than the uptake for all other particle sizes. Characterization of the silver particles by TEM and XRD show that the N_{35} and N_{Bulk} silver particles were similar in terms of particle size measurements, whereas the N_{10} silver particles were markedly smaller, suggesting that smaller particles show a greater propensity to associate with/enter into gill tissue than larger particles. TEM images on gill tissue from trout exposed to N_{10} particles showed the presence of silver particles. However, from the imaging alone, we cannot be definitive as to whether the particles detected were on the surface of the pavement cells or were incorporated into them. EDX analysis did not detect silver in the gills, likely, because

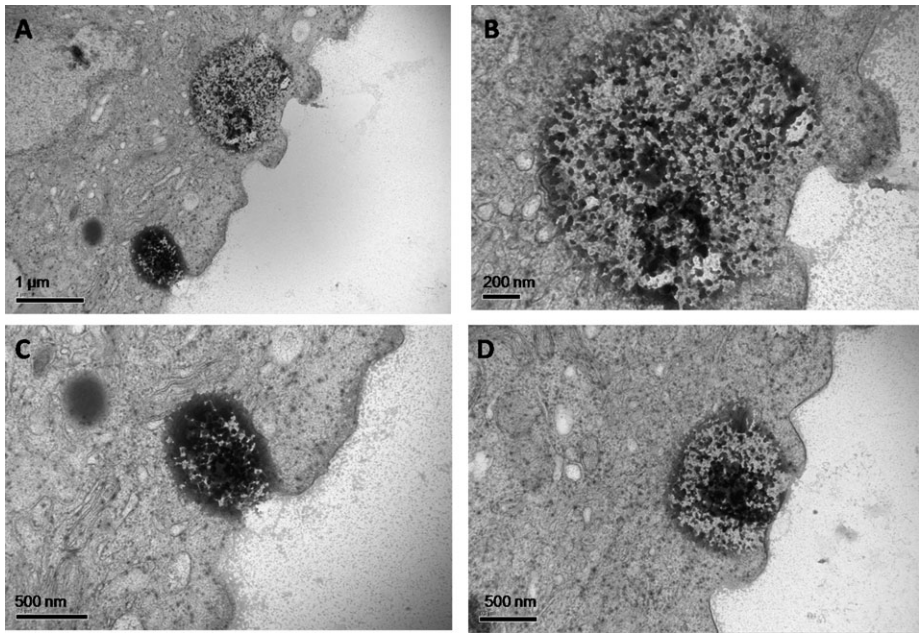

FIG. 5. TEM images of gill tissue dissected from rainbow trout after waterborne exposure to 100 µg/l N_{10} silver particles for 10 days. Images (A) and (D) show aggregates at the edges of the gill tissue, images (B) and (C) are higher magnification images of aggregates in image (A).

concentrations were not sufficiently high to be able to do so, but their presence was supported by the ICP-OES measurements (< 1 µg/g). The fact that the liver content of silver was twice that of the gills would suggest transport across the gills (see also later discussion). Assuming that there is 1% solubility of Ag in the exposure media (Fabrega *et al.*, 2009; Navarro *et al.*, 2008), uptake of silver in gills of fish exposed to the low dose of Ag NPs, at least, cannot be explained by NP dissolution and uptake of dissolved Ag, further indicating that some uptake of Ag NPs must have occurred.

Despite the association/uptake of silver with/into the gill tissue, there was no obvious damage to the gill filaments as a result of the exposures to silver particles, although some low level damage was noted in the gills of fish exposed to $AgNO_3$. Griffitt *et al.* (2009) similarly found that more silver associated with the gills of zebrafish exposed to silver NPs compared with fish exposed to soluble silver ($AgNO_3$). In that study, significant thickening of the gill lamellae was observed in fish exposed to $AgNO_3$, whereas concentrations of 1000 µg 27-nm silver particles/l did not elicit any changes in gill lamellar thickness (for a 48-h exposure). The effective doses of silver particles for inducing gill lamellar disruptions in the study by Griffitt *et al.* (2009) were, however, between 10- and 100-fold higher than in our study, and this likely explains the differences in the effects observed.

The levels of silver present in the liver of fish exposed to the high concentrations of all the particle sizes were approximately twice the concentrations in the gills per gram of tissue, suggesting that transportation of silver occurs within the blood from the sites of uptake. Contrasting with findings in the gills (where the amount of silver measured was highest for the 10-nm high-exposure regime), both N_{10} silver and N_{Bulk} silver particles showed the highest accumulation in the liver tissue. It is difficult to equate the tissue levels of N_{10} silver or N_{Bulk} silver in the liver with those in the gills, indicating a possible alternative uptake route. Indeed, it may be the case that uptake of N_{Bulk} silver (and nano silver also) was not principally via the gills but rather via the gut as a function of drinking and/or feeding on aggregated material (the fish were not fed for the exposure period). The feeding on aggregated materials that accumulate on the bottom of the tank has reported previously for aqueous exposures to other nanomaterials (Johnston *et al.*, 2010).

Although there was a twofold difference in uptake of N_{10} Ag particles in the gills between the low- and the high-dose exposures, in none of the gill samples where uptake occurred, was the concentration of Ag in the gill 10 times higher for the high dose than for the low dose. This might be explained by lowered bioavailability of Ag ENPs in the water column as a result of increased propensity for particle aggregation at higher NP concentrations as has shown in previous studies (Johnston *et al.*, 2010). The difference in uptake of N_{35} Ag in the liver of fish between the high- and low-dose exposures is close to 10-fold, however, further suggesting differences in route of uptake of Ag NPs between gill and liver tissue and that uptake into the liver as a result of fish feeding on Ag NP aggregates from the tank floor may be an important consideration.

The mechanism by which electrolytes, metal ions, and organic molecules are taken up across epithelial cell layers is

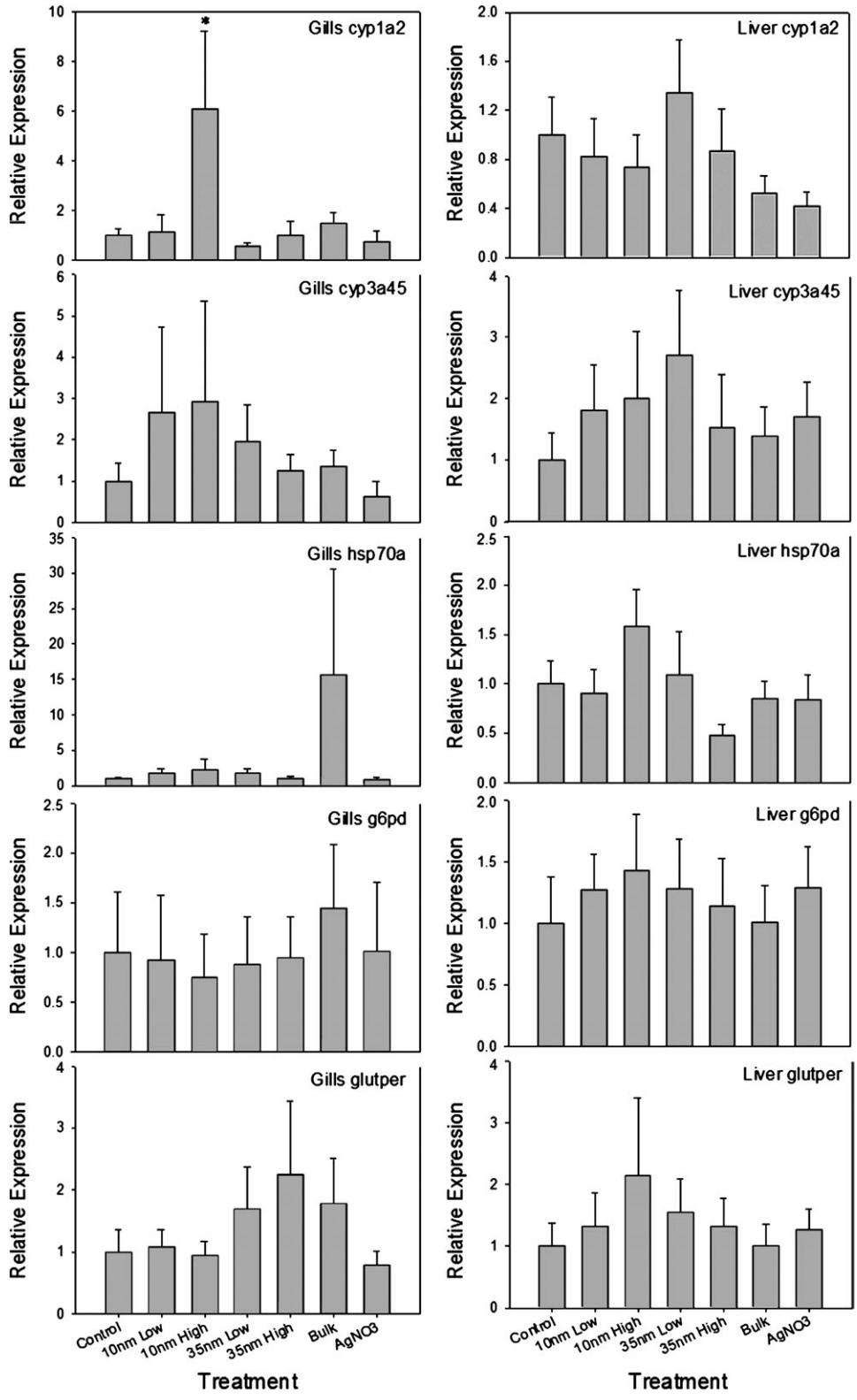

FIG. 6. Expression of *cyp1a2*, *cyp3a45*, *hsp70a*, *g6pd*, and *gpx* in gills and liver as determined by real-time PCR. Results are represented as means ± SE expressed as fold increase in relative mRNA expression (gene of interest: *rpl8*). Experimental groups consisted of eight fish and each fish was analyzed in triplicate. *Statistically significant differences in the expression levels (compared to controls) (ANOVA $p < 0.025$).

well described (Handy and Eddy, 2004). *In vivo*, both the gill and the gut surfaces are surrounded by aqueous media, which contributes to an unstirred aqueous layer above the epithelium. This layer can exchange these molecules with the mucus layer covering the epithelium, which in turn can present the molecules to the apical surface of the epithelium where uptake may occur. It is not known, however, how well this model can be applied to NPs and their uptake or how the physicochemical characteristics of the particles such as size, shape, and surface charge and the interaction of particles with the aqueous media might affect uptake. Furthermore, it is not known how this may influence release of silver ions from the particles. Our results suggest, however, that distinct differences may exist between the interaction of different sized silver particles with epithelial membranes and also with the interaction of silver particles with different epithelial surfaces, i.e., the gut and gill. As Navarro *et al.* (2008) showed in their work with *C. reinhardtii* interaction with particles with biological membranes enhanced the release of Ag^{+} from the particles; however, whether or not this phenomena is also observed in interactions between silver particles and epithelial membranes in fish is not yet known.

Levels of MDA were shown to be significantly increased only in the plasma samples of fish exposed to $AgNO_3$, suggesting that some ionic silver was entering the blood stream via the gills and/or the gut epithelium and causing lipid peroxidation. Levels of MDA in the livers of these fish, however, were significantly lower than in control fish, and this was in accordance with a lack of evidence of silver uptake into the livers for the $AgNO_3$ exposure. The apparent reduction of lipid peroxidation in the gills of fish exposed to the high concentration of N_{10} silver, despite a large accumulation of silver in the gills, is a surprising finding and is in marked contrast with several studies, which demonstrate the potential for silver NPs to generate ROS and cause oxidative stress. Rahman *et al.* (2009) found that 25-nm silver particles induced the expression of oxidative stress–related genes in the mouse brain after iv injection of 100, 500, and 1000 mg/kg, and *in vitro* studies have shown that silver NPs have the capacity to generate ROS (Carlson *et al.*, 2008; Hsin *et al.*, 2008) and cause increased lipid peroxidation (Arora *et al.*, 2008). Both liver and gill tissues have the ability to upregulate survival genes and DNA repair mechanisms (Diehl, 2000; Hansen *et al.*, 1996) when an organism is exposed to environmental stressors, which may also explain the reduced lipid peroxidation seen in response to $AgNO_3$ in the liver and to the high concentration of 10-nm Ag particles in the gills. However, if the solubility of Ag in water is taken to be 1% (Fabrega *et al.*, 2009; Navarro *et al.*, 2008), we would expect to see similar responses in the blood plasma of fish exposed to low concentrations of Ag NPs as in the exposure to $AgNO_3$. The absence of such a response may suggest that differences in dissolution rates exist between different preparations of Ag NPs.

It has been suggested that the mucus layer surrounding the gill epithelia may act as a barrier preventing NP uptake by the gills (Handy *et al.*, 2008a), and a study by Smith *et al.* (2007) demonstrated that carbon nanotubes readily associate and became trapped within mucus on the gill surface. If the silver NPs are similarly associated with the mucus on the gills for aqueous exposures, reducing/preventing penetration into the gill epithelia, this would explain the lack of any lipid peroxidation in our exposures. Interestingly, Derksen *et al.* (1998) demonstrated, under normal oxygen level conditions (dissolved oxygen = 9.5 mg/l), that particulate matter associated with the gills was effectively cleared from the gills of rainbow trout within 40 h; however, both elevated and reduced oxygen levels (25 and 4.5 mg/l, respectively) caused significantly reduced clearance of particulate matter, in resulting altered behavior normally associated with respiratory stress. It is quite possible, therefore, that the length of time that NPs are associated with the gill via the mucus before being cleared might influence vesicular uptake or oxidative stress in the gill tissue.

The suite of five genes analyzed by real-time PCR were chosen as genes representing a range of toxicity mechanisms (principally for heavy metals) in living cells. The cytochrome P450 monooxygenase system plays an important role in the detoxification of both endogenous and exogenous chemicals in animals and in fish, and they have often been used as biomarkers for environmental contamination (Råbergh *et al.*, 2000). Both *cyp1a2* and *cyp3a45* have been shown to have roles in the oxidative metabolism of exogenous compounds in rainbow trout (Lee and Buhler, 2003; Råbergh *et al.*, 2000). The expression of heat-shock proteins is associated with a general shock response, which is universally conserved throughout the animal kingdom. Measurement of heat-shock protein induction, in particular *hsp70*, has been proposed as a useful technique in toxicological screening and environmental monitoring as a variety of stressors including heavy metals, teratogens, anoxia, and heat have been shown to induce synthesis. Williams *et al.* (1996) showed that accumulation of HSP70 in the gills of juvenile rainbow trout occurred as a result of exposure to cadmium, copper, lead, and zinc via the water and via the diet. Both the glucose-6-phosphate dehydrogenase (G6PD) and the glutathione peroxidase (GPX) enzyme family play significant roles in protecting cells from oxidative damage, and measurement of their activity is commonly used as markers for oxidative stress. Both genes have multiple metal response elements in their 5′-flanking region, which has been proposed as the reason for their responsiveness to metals (Walker *et al.*, 2007). Exposure of brown trout (*Salmo trutta*) to both cadmium and copper via the water have been shown to induce expression of *gpx* messenger RNA (mRNA) (Hansen *et al.*, 2006, 2007), and both *g6pd* and *gpx* have been shown to be responsive to zinc in the gills of rainbow trout (Walker *et al.*, 2007). Thus, the genes selected for study represented a wide range of toxicological effect pathways. Interestingly, only the expression of *cyp1a2* was found to be significantly altered and this only occurred in the gills of fish exposed to the high

concentration of 10-nm silver particles, correlating with the highest level of accumulation of silver in the gills in this treatment group. Griffitt *et al.* (2009), adopting a transcriptomic approach, found that none of our targeted genes were differentially expressed in the gills of zebrafish exposed to silver NPs (26 nm, 1000 μg/l). A study by Rahman *et al.* (2009) found that exposure of rats to silver NPs caused significant downregulation of *Gpx2* in the brain frontal cortex and upregulation of *Gpx3* in the caudate nucleus. The doses of silver NPs eliciting these responses, however, were between 500 and 1000 mg/kg and are ~1000-fold higher than the maximum concentration of NPs adopted in our experiment.

Silver ions have been shown to be toxic to fish, inhibiting carbonic anhydrase activity leading to a net loss of Na^+ and Cl^- across the gills and inhibiting Na^+/K^+ ATPase activity (Morgan *et al.*, 1997). The toxic effects of silver ions are due to their interaction at the gill surface and not as a result of internal silver accumulation (Wood *et al.*, 1996b). We, therefore, might have expected exposure to $AgNO_3$ to alter the expression of some of these genes in the gills. ICP-OES employed in this study cannot distinguish between different valence states of metals. Although previous studies have established that Ag solubility in water is ~1% (Fabrega *et al.*, 2009; Navarro *et al.*, 2008), in our experiment, it is not known what proportion (if any) of the silver present in the Ag NP exposure media was in the form of Ag^+. Furthermore, it is not known in what form silver was associated with the gills or transported to the liver. The lack of any effect, however, is likely explained by the low exposure concentrations adopted (chosen to reflect a 10-fold lower concentration than the accepted 96 h LC_{50} value for rainbow trout) and effective repair mechanisms in these tissues.

The known toxicity of silver ions has led to the proposal in a number of studies that release of silver ions (Ag^+) from silver NPs could be in part responsible for toxic responses seen in exposures to silver NPs (e.g., Navarro *et al.*, 2008). This idea, however, conflicts with the known stability of zero-valent silver in water. Griffitt *et al.* (2009) conducted concurrent exposures of zebrafish to silver NPs and Ag^+ at concentrations that matched the amount of silver ions released by the NPs. Dissolved silver from NPs was measured and found to be 0.07% of the silver NP mass. The method used, however, does not specifically elucidate whether the silver present was ionic or very small zero-valent silver NPs. This may explain why gill damage was observed in Ag^+ exposures but not in silver NP exposures. Also the gill global gene expression patterns between these exposures differed markedly from each other, suggesting that toxicity mechanisms differed between treatments.

CONCLUSION

Our results show that smaller NP sizes have a greater propensity to associate with the gills of rainbow trout but that the mucus layer on the gills may be an effective barrier to entry of the NPs into the gill cells. However, induction of *cyp1a2* in the gills of fish exposed to high concentrations of N_{10} silver particles may be indicative of oxidative metabolism in response to the exposure. At this time, it is difficult to speculate on the mechanism of action of *cyp1a2* in the gills as it is unknown whether the effects seen are as a result of exposure to the silver NPs, silver ions, or a combination of both. We show evidence of lipid peroxidation in the plasma of fish exposed to $AgNO_3$; however, there was an apparent decreased lipid peroxidation in the gills of fish exposed to high concentrations of N_{10} silver particles. Uptake of silver particles was demonstrated in the liver but with no differences in uptake relative to particle size. Liver burden of silver was approximately twice that seen in gills, suggesting that the gut epithelium may be an important route of exposure for silver particles to fish. These results suggest that both the size of the NP and the type of epithelium where NPs are presented affect their uptake. The importance of Ag^+ as the mechanism of silver NP toxicity needs further investigation and accurate measurements of the proportions of zero-valent silver and Ag^+ (and Ag^+ sorbed to NP surfaces) for the different sized NPs would be needed to do this. Care should also be taken when defining dissolved silver. Ag^+ in solution and stable suspensions of zero-valent silver NPs are distinctly different but have both been described in the literature as solutions. Our findings also revealed that for all three particle types, size and surface area measurements differed considerably to the information given by the manufacturers, emphasizing the need for rigorous characterization of particles to ascertain the nature of the particles to which the test organisms are exposed. Our results show that exposure of silver NPs to rainbow trout at concentrations close to current estimations of environmental levels can result in accumulation of silver in the gills and liver of fish and can affect likely oxidative metabolism in the gills.

FUNDING

Natural Environment Research Council (NER/S/A/2005/13319 studentship, NE/D004942/1, NE/C002369/1, NE/G01113/1, NE/E008429/1); Environment Agency, UK, to C.R.T., R.A., V.S., and J.L.

ACKNOWLEDGMENTS

We would like to thank Kevin Brigden, of Greenpeace Research Laboratories in Exeter, for help with ICP-OES analysis and Pete Splatt and Gavin Wakely in the Bioimaging Suite at the University of Exeter. All animal procedures were performed in accordance with the Animals (Scientific Procedures) Act, 1986 (UK). The Natural Environment Research Council Facility for Environmental Nanoparticle Analysis and Characterisation is acknowledged for help with characterization.

REFERENCES

Arora, S., Jain, J., Rajwade, J. M., and Paknikar, K. M. (2008). Cellular responses induced by silver nanoparticles: in vitro studies. *Toxicol. Lett.* **179,** 93–100.

Asharani, P. V., Wu, Y. L., Gong, Z., and Valiyaveettil, S. (2008). Toxicity of silver nanoparticles in zebrafish models. *Nanotechnology* **19,** 2255102–2255107.

Baalousha, M., Manciulea, A., Cumberland, S., Kendall, K., and Lead, J. R. (2008). Aggregation and surface properties of iron oxide nanoparticles: influence of pH and natural organic matter. *Environ. Toxicol. Chem.* **27,** 1875–1882.

Benn, T. M., and Westerhoff, P. (2008). Nanoparticle silver released into water from commercially available sock fabrics. *Environ. Sci. Technol.* **42,** 4133–4139.

Braydich-Stolle, L., Hussain, S., Schlager, J. J., and Hofmann, M.-C. (2005). In vitro cytotoxicity of nanoparticles in mammalian germline stem cells. *Toxicol. Sci.* **88,** 412–419.

Carlson, C., Schrand, A. M., Braydich-Stolle, L. K., Hess, K. L., Jones, R. L., Schlager, J. J., and Hussain, S. M. (2008). Unique cellular interaction of silver nanoparticles: size-dependent generation of reactive oxygen species. *J. Phys. Chem. B* **112,** 13608–13619.

Chen, X., and Schluesener, H. J. (2008). Nanosilver: a nanoproduct in medical application. *Toxicol. Lett.* **176,** 1–12.

Choi, O., Deng, K. K., Kim, N.-J., Ross, L., Jr, Surampalli, R. Y., and Hu, Z. (2008). The inhibitory effects of silver nanoparticles, silver ions, and silver chloride colloids on microbial growth. *Water Res.* **42,** 3066–3074.

Conner, E., Margulies, R., Liu, M., Smilen, S. W., Porges, R. F., and Kwon, C. (2006). Vaginal delivery and serum markers of ischemia/reperfusion injury. *Int J Gynaecol Obstet.* **94,** 96–102.

Derjaguin, B. V., and Landau, L. D. (1941). Theory of the stability of strongly charged lyophobic sols and of the adhesion of strongly charged particles in solutions of electrolytes. *Acta Phys. Chim. URSS* **14,** 633–662.

Derksen, J. A., Ostland, V. E., and Ferguson, H. W. (1998). Particle clearance from the gills of rainbow trout (Oncorhynchus mykiss). *J. Comp. Pathol.* **118,** 245–256.

Diehl, A. M. (2000). Cytokine regulation of liver injury and repair. *Immunol. Rev.* **174,** 160–171.

Domingos, R. F., Baalousha, M. A., Ju-Nam, Y., Reid, M. M., Tufankji, N., Lead, J. R., Leppard, G. G., and Wilkinson, K. J. (2009). Characterizing manufactured nanoparticles in the environment: multimethod determination of particle sizes. *Environ. Sci. Technol.* **43,** 7277–7284.

Fabrega, J., Fawcett, S. R., Renshaw, J. C., and Lead, J. R. (2009). Silver nanoparticle impact on bacterial growth: effect of pH, concentration, and organic matter. *Environ. Sci. Technol.* **43,** 7285–7290.

Filby, A. L., and Tyler, C. R. (2005). Molecular characterization of estrogen receptors 1, 2a, and 2b and their tissue and ontogenic expression profiles in fathead minnow (*Pimephales promelas*). *Biol. Reprod.* **73,** 648–662.

Griffitt, R. J., Hyndman, K., Denslow, N. D., and Barber, D. S. (2009). Comparison of molecular and histological changes in zebrafish gills exposed to metallic nanoparticles. *Toxicol. Sci.* **107,** 404–415.

Handy, R. D., and Eddy, F. B. (2004). Transport of solutes across biological membranes in eukaryotes: an environmental perspective. In *Physicochemical kinetics and transport at chemical-biological interfaces* (H. P. van Leeuwen and W. Köster, Eds.), pp. 337–356. Wiley, Chichester, UK.

Handy, R. D., Henry, T. B., Scown, T. M., Johnston, B. D., and Tyler, C. R. (2008a). Manufactured nanoparticles: their uptake and effects on fish-a mechanistic analysis. *Ecotoxicology* **17,** 396–409.

Handy, R. D., Owen, R., and Valsami-Jones, E. (2008b). The ecotoxicology of nanoparticles and nanomaterials: current status, knowledge gaps, challenges, and future needs. *Ecotoxicology* **17,** 315–325.

Hansen, B. H., Rømma, S., Garmo, O. A., Pedersen, S. A., Olsvik, P. A., and Andersen, R. A. (2007). Induction and activity of oxidative stress-related proteins during waterborne Cd/Zn-exposure in brown trout (Salmo trutta). *Chemosphere* **67,** 2241–2249.

Hansen, B. H., Romma, S., Softeland, L. I. R., Olsvik, P. A., and Andersen, R. A. (2006). Induction and activity of oxidative stress-related proteins during waterborne Cu-exposure in brown trout (Salmo trutta). *Chemosphere* **65,** 1707–1714.

Hansen, H. J. M., Olsen, A. G., and Rosenkilde, P. (1996). The effect of Cu on gill and esophagus lipid metabolism in the rainbow trout (Oncorhynchus mykiss). *Comp. Biochem. Phys.* **113C,** 23–29.

Hsin, Y.-H., Chen, C.-F., Huang, S., Shih, T.-S., Lai, P.-S., and Chueh, P. J. (2008). The apoptotic effect of nanosilver is mediated by a ROS- and JNK-dependent mechanism involving the mitochondrial pathway in NIH3T3 cells. *Toxicol. Lett.* **179,** 130–139.

Hussain, S. M., Hess, K. L., Gearhart, J. M., Geiss, K. T., and Schlager, J. J. (2005). In vitro toxicity of nanoparticles in BRL 3A rat liver cells. *Toxicol. In Vitro* **19,** 975–983.

Inoue, K. I., Takano, H., Yanagisawa, R., Koike, E., and Shimada, A. (2009). Size effects of latex nanomaterials on lung inflammation in mice. *Toxicol. Appl. Pharmacol.* **234,** 68–76.

Jayesh, P., Chatterjeec, A. K., Duttaguptab, S. P., and Mukherji, S. (2008). Strain specificity in antimicrobial activity of silver and copper nanoparticles. *Acta Biomater.* **4,** 707–716.

Johnston, B. D., Scown, T. M., Moger, J., Cumberland, S., Baalousha, M., Linge, K., van Aerle, R., Jarvis, K., Lead, J. R., and Tyler, C. R. (2010). Bioavailability of nanoscale metal oxides, TiO2, CeO2, and ZnO to fish. *Environ. Sci. Technol.* **44,** 1144–1151.

Jung, W. K., Kim, S. H., Koo, H. C., Shin, S., Kim, J. M., Park, Y. K., Hwang, S. Y., Yang, H., and Park, Y. H. (2007). Antifungal activity of the silver ion against contaminated fabric. *Mycoses* **50,** 265–269.

Kumar, P. S. S., Sivakumar, R., Anandan, S., Madhavan, J., Maruthamuthu, P., and Ashokkumar, M. (2008). Photocatalytic degradation of Acid Red 88 using Au–TiO2 nanoparticles in aqueous solutions. *Water Res.* **42,** 4878–4884.

Larese, F. F., D'Agostin, F., Crosera, M., Adami, G., Renzi, N., Bovenzi, M., and Maina, G. (2009). Human skin penetration of silver nanoparticles through intact and damaged skin. *Toxicology* **255,** 33–37.

Lee, K. J., Nallathamby, P. D., Browning, L. M., Osgood, C. J., and Xu, X.-H. N. (2007). *In vivo* imaging of transport and biocompatibility of single silver nanoparticles in early development of zebrafish embryos. *ACS Nano* **1,** 133–143.

Lee, S.-J., and Buhler, D. R. (2003). Cloning, tissue distribution, and functional studies of a new cytochrome P450 3A subfamily member, CYP3A45, from rainbow trout (Oncorhynchus mykiss) intestinal ceca. *Arch. Biochem. Biophys.* **412,** 77–89.

Li, Q. L., Mahendra, S., Lyon, D. Y., Brunet, L., Liga, M. V., Li, D., and Alvarez, P. J. J. (2008). Antimicrobial nanomaterials for water disinfection and microbial control: potential applications and implications. *Water Res.* **42,** 4591–4602.

Luoma, S. N. (2008). *Silver nanotechnologies and the environment: old problems or new challenges?* Woodrow Wilson International Centre for Scholars: Project on Emerging Nanotechnologies, Washington, DC.

Mayer, G. D., Leach, A., Kling, P., Olsson, P.-E., and Hogstrand, C. (2003). Activation of the rainbow trout metallothionein—a promoter by silver and zinc. *Comp. Biochem. Physiol. Part B Biochem. Mol. Biol.* **134,** 181–188.

Morgan, I. J., Henry, R. P., and Wood, C. M. (1997). The mechanism of acute silver nitrate toxicity in freshwater rainbow trout (Oncorhynchus mykiss) is inhibition of gill Na+ and Cl- transport. *Aquat. Toxicol.* **38,** 145–163.

Navarro, E., Piccapietra, F., Wagner, B., Marconi, F., Kaegi, R., Odzak, N., Sigg, L., and Behra, R. (2008). Toxicity of silver nanoparticles to Chlamydomonas reinhardtii. *Environ. Sci. Technol.* **42,** 8959–8964.

Park, S., Lee, Y. K., Jung, M., Kim, K. H., Chung, N., Ahn, E.-K., Lim, Y., and Lee, K.-H. (2007). Cellular toxicity of various inhalable metal nanopartciles on human alveolar epithelial cells. *Inhal. Toxicol.* **19,** 59–65.

Perelshtein, I., Applerot, G., Perkas, N., Guibert, G., Mikhailov, S., and Gedanken, A. (2008). Sonochemical coating of silver nanoparticles on textile fabrics (nylon, polyester and cotton) and their antibacterial activity. *Nanotechnology* **19,** 245705.

Råbergh, C. M. I., Vrolijk, N. H., Lipsky, M. M., and Chen, T. T. (2000). Differential expression of two cyp1a genes in rainbow trout (*Oncorhynchys mykiss*). *Toxicol. Appl. Pharmacol.* **165,** 195–205.

Rahman, M. F., Wang, J., Patterson, T. A., Saini, U. T., Robinson, B. L., Newport, G. D., Murdock, R. C., Schlager, J. J., Hussain, S. M., and Ali, S. F. (2009). Expression of genes related to oxidative stress in the mouse brain after exposure to silver-25 nanoparticles. *Toxicol. Lett.* **187,** 15–21.

Schrand, A. M., Braydich-Stolle, L. K., Schlager, J. J., Dai, L., and Hussain, S. M. (2008). Can silver nanoparticles be useful as potential biological labels? *Nanotechnology* **19,** 235104.

Smith, C. J., Shaw, B. J., and Handy, R. D. (2007). Toxicity of single walled carbon nanotubes on rainbow trout, (*Oncorhynchus mykiss*): respiratory toxicity, organ pathologies, and other physiological effects. *Aquat. Toxicol.* **82,** 93–109.

Sun, L., Singh, A. K., Vig, K., Pillai, S. R., and Singh, S. R. (2008). Silver nanoparticles inhibit replication of respiratory syncytial virus. *J. Biomed. Nanotechnol.* **4,** 149–158.

Verwey, E. J. W., and Overbeek, J. T. G. (1948). *Theory of the Stability of Lyophobic Colloids*. Elsevier, Amsterdam, UK.

Walker, P. A., Bury, N. R., and Hogstrand, C. (2007). Influence of culture conditions on metal-induced responses in a cultured rainbow trout gill epithelium. *Environ. Sci. Technol.* **41,** 6505–6513.

Walker, P. A., Kille, P., Hurley, A., Bury, N. R., and Hogstrand, C. (2008). An in vitro method to assess toxicity of waterborne metals to fish. *Toxicol. Appl. Pharmacol.* **230,** 67–77.

Wang, H.-T., Nafday, O. A., Haamheim, J. R., Tevaarwerk, E., Amro, N. A., Sanedrin, R. G., Chang, C.-Y., Ren, F., and Pearton, S. J. (2008). Toward conductive traces: Dip Pen Nanolithography of silver nanoparticle-based inks. *Appl. Phys. Lett.* **93,** 143105.

Warheit, D. B., Webb, T. R., Colvin, V. L., Reed, K. L., and Sayes, C. M. (2007). Pulmonary bioassay studies with nanoscale and fine-quartz particles in rats: toxicity is not dependent upon particle size but on surface characteristics. *Toxicol. Sci.* **95,** 270–280.

Warheit, D. B., Webb, T. R., Sayes, C. M., Colvin, V. L., and Reed, K. L. (2006). Pulmonary instillation studies with nanoscale TiO_2 rods and dots in rats: toxicity is not dependent upon particle size and surface area. *Toxicol. Sci.* **91,** 227–236.

Wilkinson, K. J., Balnois, E., Leppard, G. G., and Buffle, J. (1999). Characteristic features of the major components of freshwater colloidal organic matter revealed by transmission electron and atomic force microscopy. *Colloids Surf. Physicochem. Eng. Aspects* **155,** 287–310.

Williams, J. H., Farag, A. M., Stansbury, M. A., Young, P. A., Bergman, H. L., and Petersen, N. S. (1996). Accumulation of hsp70 in juvenile and adult rainbow trout gill exposed to metal-contaminated water and/or diet. *Environ. Toxicol. Chem.* **15,** 1324–1328.

Wood, C. M., Hogstrand, C., Galvez, F., and Munger, R. S. (1996a). The physiology of waterborne silver toxicity in freshwater rainbow trout (Oncorhynchus mykiss) 1. The effects of ionic Ag+. *Aquat. Toxicol.* **35,** 93–109.

Wood, C. M., Hogstrand, C., Galvez, F., and Munger, R. S. (1996b). The physiology of waterborne silver toxicity in freshwater rainbow trout (Oncorhynchus mykiss) 2. The effects of silver thiosulfate. *Aquat. Toxicol.* **35,** 111–125.

Yeo, M. K., and Kang, M. (2008). Effects of nanometer sized silver materials on biological toxicity during zebrafish embryogenesis. *Bull. Korean Chem. Soc.* **29,** 1179–1184.